Journal of Sensor Science and Technology
Vol. 32, No. 6 (2023) pp. 418-424
http://dx.doi.org/10.46670/JSST.2023.32.6.418
pISSN 1225-5475/eISSN 2093-7563

Ultrasonic Targeting of NK Cell in Vessel Bifurcation for Immunotherapy: Simulation and Experimental Validation

Saqib Sharif[1,2], Hyeong-Woo Song[2], Daewon Jung[2], Hiep Xuan Cao[2], Jong-Oh Park[2], Byungjeon Kang[2,3,4,+], and Eunpyo Choi[1,2,3,+]

Abstract

Natural killer (NK) cells play a crucial role in combating infections and tumors. However, their therapeutic application in solid tumors is hindered by challenges, such as limited lifespan, tumor penetration, and delivery precision. Our research introduces a novel ultrasonic actuation technique to navigate NK cells more effectively in the vascular system, particularly at vessel bifurcations where targeted delivery is most problematic. We use a hemispherical ultrasonic transducer array that generates phase-modulated traveling waves, focusing on an ultrasound beam to steer NK cells using blood-flow dynamics and a focused acoustic field. This method enables the precise obstruction of non-target vessels and efficiently directs NK cells toward the tumor site. The simulation results offer insights into the behavior of NK cells under various conditions of cell size, radiation pressure, and fluid velocity, which inform the optimization of their trajectories and increase targeting efficiency. The experimental results demonstrate the feasibility of this ultrasonic approach for enhancing NK cell targeting, suggesting a potential leap forward in solid tumor immunotherapy. This study represents a significant step in NK cell therapeutic strategies, offering a viable solution to the existing limitations and promising enhancement of the efficacy of cancer treatments.

Keywords: Ultrasonic manipulation, NK Cell, Immunotherapy, Acoustic radiation force, Targeted drug delivery

1. INTRODUCTION

Imposing an ultrasound field on a fluid with suspended particles induces acoustic scattering owing to the differences in sound speed and density between the particles and surrounding fluid, resulting in an acoustic radiation force (ARF) on the particles. This phenomenon, known as acoustophoresis, utilizes acoustophoretic force to manipulate particles, including cells, microorganisms, and microbubbles. Such manipulation is crucial for on-chip microparticle management and acoustic navigation of microparticles in complex fluid flows [1].

Over the past few decades, ultrasound has been widely studied for imaging and therapeutic purposes. For instance, high-intensity focused ultrasound has been employed in cancer therapy [2-4], while shock wave lithotripsy (SWL) is routinely used to disintegrate kidney stones [5-7]. Ultrasound has also been reported to enhance thrombolysis in deep vein thrombosis (DVT) [8] and increase drug permeability through the skin [9]. The development of multiarray transducers has spurred interest in using ultrasound for targeted drug delivery, particularly for the trapping and navigation/blocking of drug carriers, such as drug-loaded liposomes, microbubbles carrying drugs, and cytokine transfection [10-15].

Immune cell therapies, including CAR T-cell and NK cell therapies, have shown success in treating hematological malignancies, such as lymphomas and leukemias [16-20]. Notably, HLA-mismatched NK cells offer a viable treatment without the risk of graft-versus-host disease (GVHD), with extensive clinical use indicating safety and a minimal risk of cytokine release syndrome (CRS) [21,22]. However, navigating these cells within the cardiovascular system remains challenging because of their size, density, and compressibility.

This article introduces an acoustic manipulation system designed to direct natural killer (NK) cells into fluid flow and through vessel bifurcations. The system leverages hydrodynamic

[1]School of Mechanical Engineering, Chonnam National University
Gwangju 61186, Korea
[2]Korea Institute of Medical Microrobotics, Gwangju 61011, Korea
[3]College of AI Convergence, Chonnam National University
Gwangju 61186, Korea
[4]Graduate School of Data Science, Chonnam National University
Gwangju 61186, Korea
[+]Corresponding author: bjkang8204@jnu.ac.kr, eunpyochoi@jnu.ac.kr
(Received: Nov. 13, 2023, Revised: Nov. 15, 2023, Accepted: Nov. 17, 2023)

drag as the primary carrier force, supplemented by acoustic pressure, to guide the cells toward the target. Our simulations utilized a 30-transducer acoustic actuator operating at 1 MHz, capable of generating a focused beam at the center of the array, demonstrating a novel technique for NK cell delivery.

2. THEORY AND METHODS

2.1 Generation of focused US beam

The ultrasound navigation system was developed with 30 transducers, and each transducer signal was modulated using a custom control system. A Schematic of the US actuator is depicted in Fig. 1. To compute the acoustic field, we utilized a far-field piston source with single-frequency emissions controlled through acceleration. The complex acoustic pressure (*P*) generated by the entire array at a specific location result from the vector summation of 30 individual complex acoustic pressures (*Pj*) contributed by each piston source emitted at a single frequency. This phenomenon can be mathematically expressed as follows [26]:

$$P = \Sigma_{j=1}^{30} P_j(r) = P_0 A \frac{D_f(\theta)}{d} e^{i(\varphi + kd)} \tag{1}$$

$$D_f = \frac{2J_1(aksin\theta)}{aksin\theta} \tag{2}$$

where P_0 denotes the transducer amplitude constant power and A denotes the peak-to-peak amplitude of the excitation signal. D_f represents a far-field directivity function based on the angle θ between the transducer normal and point r. Moreover, d denotes the propagation distance in free space, ϕ denotes the phase delay of the transducer, $k = 2\pi/\lambda$ indicates the wavenumber, J_1 represents a first-order Bessel function, and a denotes the radius of the emitting source.

2.2 Acoustic radiation force on NK Cell

Considering NK cells as spherical particles immersed in the propagating fluid, the acoustic pressure field applies a deflective force, the acoustic radiation force (ARF), on the particles. The ARF ($\vec{F}_{rad}$), which acts upon a diminutive spherical particle, is amenable to calculation by leveraging the gradient of the Gor'kov potential field, U [1, 27].

$$\vec{F}_{rad} = -\nabla U_{rad} \tag{3}$$

$$U_{rad} = \frac{4\pi}{3} R_{NK}^3 \left[f_1 \frac{1}{2} \langle P^2 \rangle - f_2 \rho_0 \frac{3}{4} \langle v^2 \rangle \right] \tag{4}$$

$$f_1 = 1 - \frac{c_0^2 \rho_0}{c_{NK}^2 \rho_{NK}} \quad \& \quad f_2 = \frac{2(\rho - 1)}{2\rho + 1} \quad \rho = \rho_{NK}/\rho_0 ,$$

where R_{NK} denotes the radius of the NK cell, ρ_0 and ρ_{NK} denote the density of fluid and NK cell, respectively, and ρ indicates the ratio of densities, c_0 and c_{NK} represent the speed of sound of fluid and NK cell, respectively. Moreover, P indicates complex pressure. The density and speed of sound in the NK cells are 1060 kg/m^3 and 1540 m/s, respectively [28,29]. The density and speed of sound of the water are 1000 kg/m^3 and 1500 m/s, respectively.

2.3 Hydrodynamic Drag Force

The ultrasound navigation system is developed using 30 transducers, and each signal of the transducers assumes that the radius R_p of the NK cell does not change. The Stokes drag force F_{drag} acting on one NK cell in the fluid is given by

$$F_{drag} = 6\pi\eta R_p (v_f - v_p) \tag{5}$$

where η denotes the dynamic viscosity of the liquid and v_f and v_p indicate the NK cell and liquid velocity, respectively. The translational motion of a NK cell is mathematically described as follows:

$$m_p \frac{\vec{dv_p}}{dt} = \overrightarrow{F_{drag}} + \overrightarrow{F_{rad}} , \tag{6}$$

where v_p and m_p denote the translational velocity and mass of the NK cell, respectively.

3. RESULTS AND DISCUSSIONS

3.1 Numerical Simulations

To assess the enhanced targeting efficiency of NK cells, we developed an idealized numerical model using the finite element software COMSOL Multiphysics. This model facilitates the coupled calculation of acoustic pressure fields, acoustic radiation force on NK cells, primary Bjerknes force on microbubbles (MB), and flow field along with particle trajectory analysis. The Y-shaped channel simulation featured inlet and outlet diameters of 3 mm and 1.5 mm, respectively, with average fluid velocity '*v*' at the inlet serving as a tunable parameter that affects the intra-vessel velocity distribution. In this study, we modeled a non-pulsatile steady flow of a weakly compressible fluid, as detailed in Table 1.

Table 1. Simulation parameters.

Name	Expression	Value
Fluid viscosity	η_f	5×10^{-3} [Pa·s]
Fluid density	ρ_f	997 [kg·m^{-3}]
NK Cell density	ρ_p	1040 [kg·m^{-3}]
NK Cell diameter	d_p	10 – 15 [μm]
Vessel diameter	D	2 [mm]
Avg. Fluid velocity	v_f	1 – 3 [mm·s^{-1}]
Number of UT array	UT	30
Resonance frequency	w_0	1 [MHz]
Controllable Voltage	V_{PP}	10 – 200 [V]
UT Array Diameter	D	75 [mm]

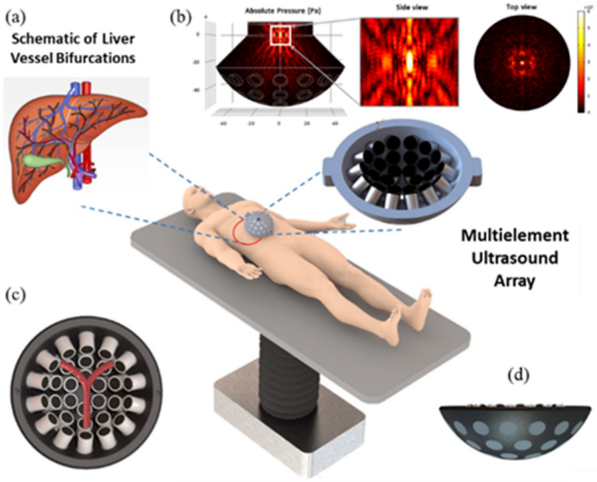

Fig. 1. Schematic concept of acoustic navigation system for controlling micro/nano carriers for targeted drug delivery in the vessel bifurcations. (a) Schematic description of liver vessel bifurcations. (b) Absolute acoustic radiation pressure field with both zoomed ZY plane and top view. (c) Animated description of Y-shaped blood vessel bifurcation surrounded on the top of 30 UT array ultrasonic actuator. (d) ZY plane lateral view of ultrasonic actuator.

To streamline the simulation process, we introduced an ensemble of 100 microparticles at the inlet in four temporal batches of 25, each matching the initial velocity "v." These particles, representing NK cells with diameters between 10–15 μm, had uniform acoustic properties, such as density and compressibility, throughout the simulation. A submerged transducer array positioned below the channel, as shown in Fig. 1, facilitates the tracking of these particles.

Neglecting the buoyancy and secondary radiation forces, we traced the time-dependent particle positions using the particle tracing module of COMSOL based on the equivalent force

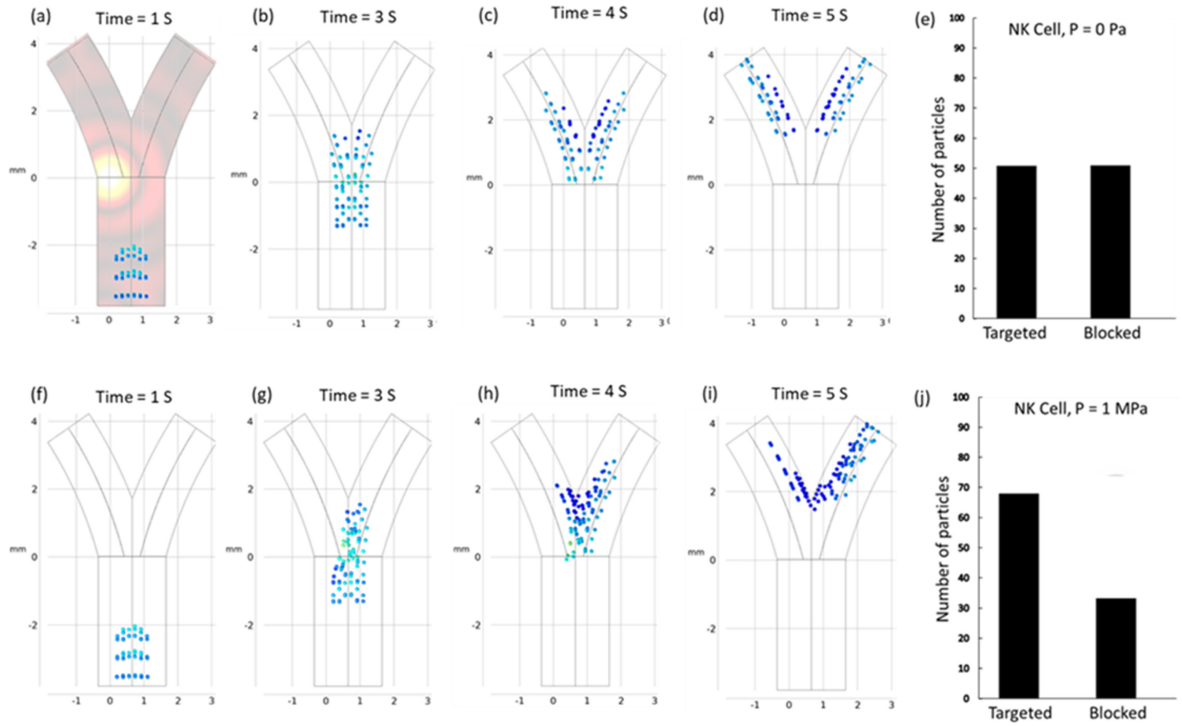

Fig. 2. (a)-(e) Simulated particle trajectories and targeting efficiency in the absence of any external acoustic field exhibit a state of uniform particle distribution within both channels. The mean velocity and particle diameter of the fluid are established at 1 mm/s and 10 μm, respectively. (f)-(j) Simulated particle trajectories and targeting efficiency in the presence of any external acoustic field, 1 MPa and 1 μm/s fluid flow.

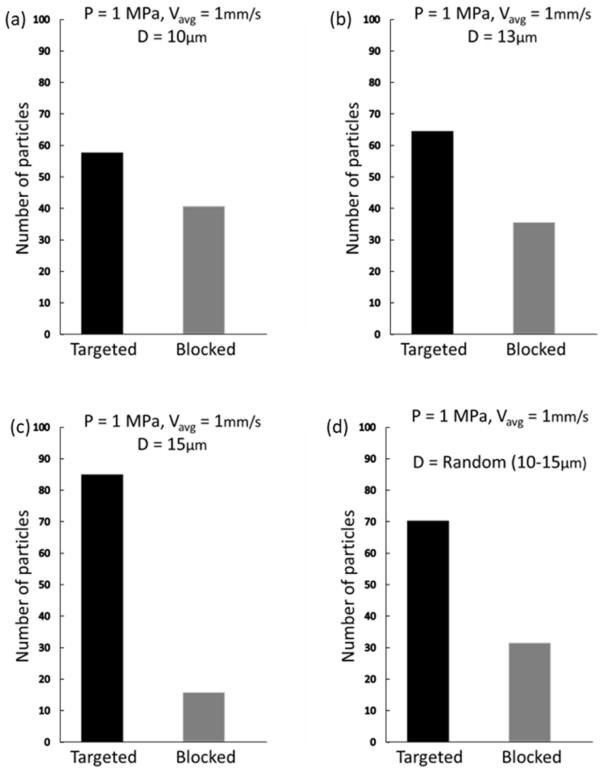

Fig. 3. Simulated target navigation efficiency dependence on the particle size. The acoustic radiation force becomes increasingly dominant as the size of NK cells increases.

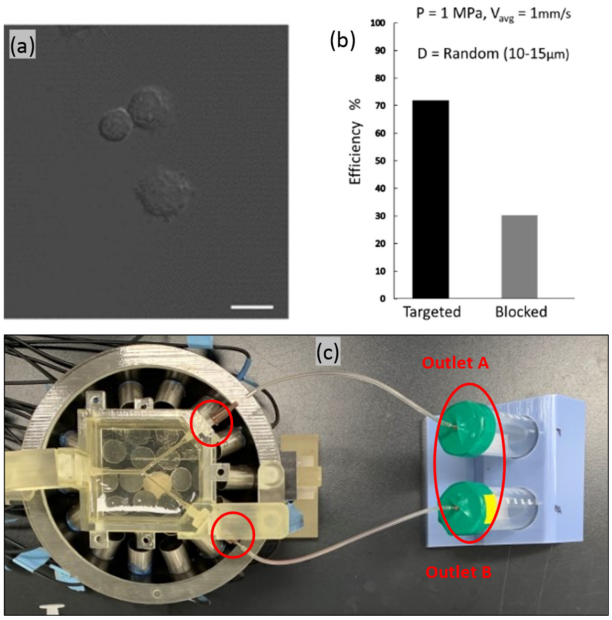

Fig. 4. (a) Confocal images of NK cells, with scale bar of 10 μm. (b) Graphs represent the experimental targeting efficiency of NK cells. (c) Phantom containing fluid channel suspended on top of the ultrasonic transducers with specified inlets and outlets.

equation (Eq. 6). The focus of the ultrasound, which is crucial for applications in microscale robotics and biomedicine, was optimized by manually adjusting the focal point of the polystyrene particles, thereby enhancing the precision of particle movement within the vessel geometry.

Fig. 2(a)-(e) depict the particle behavior without an external acoustic pressure field, where the particles primarily followed the natural drag of the fluid, leading to their uniform distribution across the channel. Interestingly, particle tracking at both outlets was performed using the particle counting function of COSMOL, with 50 particles systematically reaching each outlet.

3.2 The effect of NK cell size on navigation

The NK cells, utilized for navigation within the described phantom model, typically measure between 10–15 μm in diameter, which was verified using confocal imaging, as shown in Fig. 4(a). In our model, the diameter of the NK cells was a critical consideration, given the significant impact of particle size on their dynamic response to acoustic radiation and drag forces. Ultimately, the response influences the mobility and precision of cells in navigating within a fluid medium. Smaller particles are more amenable to manipulation, enabling more accurate control and targeting. The simulations tracked the trajectories of uniformly distributed microparticles with diameters ranging from 10–15 μm, with subsequent calculation of navigation efficiency for each size group. Fig. 3 presents a comparative analysis of these results, indicating that the efficiency is positively correlated with the particle size. However, the inherent variability of NK cell size in practical scenarios precludes size control. Confocal imaging confirmed the presence of NK cells with sizes varying randomly within the 10–15 μm range in a fluid solution. Therefore, we incorporated cells with random diameters to reflect this variation. The recalculated targeting efficiencies, depicted in Fig. 3(d), are consistent with the experimental outcomes illustrated in Fig. 4(b).

3.3 The effect of Fluid velocity on navigation

Fluid dynamics in vessel bifurcations present a formidable challenge for intravascular navigation systems because of their complexity. The primary obstacle is the variable flow patterns found in living organisms, which complicate the precision of the control mechanisms. Fluctuations in the fluid velocity of blood vessels alter the drag forces, thereby affecting micro-particle navigation. Fig. 5 illustrates this dynamic, showing the alteration in the particle trajectories at different fluid velocities. At a velocity of 2 mm/s, the targeting efficiency of the vessels drops to 40–60%

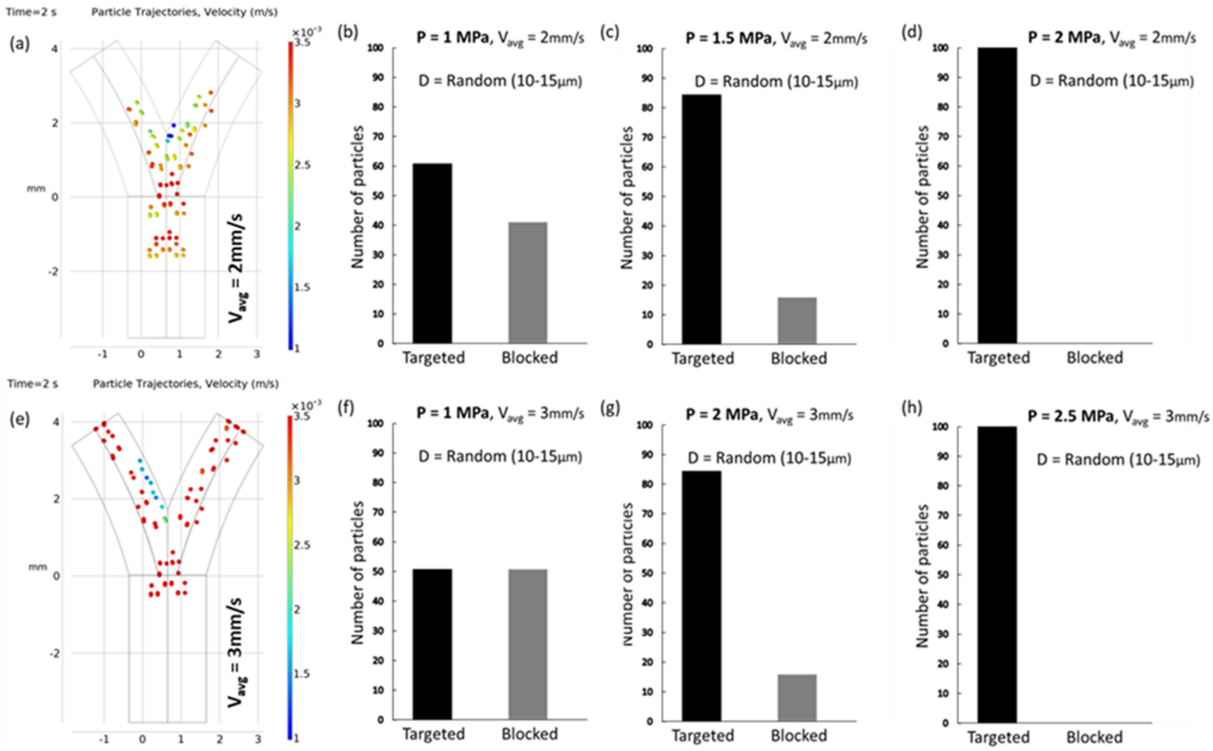

Fig. 5. (a) Simulated trajectories of particles illustrating the change in navigation efficiency as the fluid velocity increases. For 2 mm/s, the vessel blockage ratio is reduced to 40–60. (b)-(d) The graphs represent the simulated targeting efficiency of NK cells increasing with the acoustic pressure. (e) Simulated trajectories of particles for a fluid velocity of 3 mm/s. The particles move too fast to be affected by acoustic force, resulting in a targeting ratio of 48–52. (f)-(h) The graphs represent the simulated targeting efficiency of NK cells increasing with the acoustic pressure.

compared to that at 1 mm/s. This inefficiency can be addressed by increasing the acoustic pressure; however, it may affect the blood flow and cell distribution. By incrementally increasing the acoustic pressure to 1.5 MPa, we successfully directed 86 particles toward the target, with 16 particles entering the occluded area. Increasing the pressure to 2 MPa resulted in complete trajectory control, achieving 100% targeting efficiency. At a higher velocity of 3 mm/s, the particles outpaced the acoustic forces, as reflected in a targeting ratio of 48–52%. Increasing the acoustic pressure to 2 MPa enhanced the targeting efficiency by 85%. Escalating the pressure to 2.5 MPa yielded perfect efficiency. However, increasing the pressure further elevates the risk of NK cells adhering to vessel walls. Our simulations underscore the necessity of fine-tuning acoustic pressure to match specific fluid and particle conditions for successful navigation.

3.4 Controlling NK Cells in a Phantom Model

The phantom model was developed using a previously reported method [30]. It features a Y-shaped channel composed of 20% gelatin with a 2 mm diameter inlet and a 1.5 mm diameter outlet. We injected 1×10^6 NK cells into the phantom at a flow rate of 2 ml/min, which is approximately 1 mm/s, the value used in our simulations. The phantom was positioned on an array of transducers, as shown in Fig. 4(c). The actuator comprises 30 immersion-type transducers operated with signals modulated by a custom control system. The flow setup included a syringe pump and particle collector. Following a 10-minute flow period for NK cells, the output was concentrated via centrifugation and resuspended in PBS. The samples were analyzed using a microplate reader (Varioskan Flash; Thermo Fisher Scientific) at excitation and emission wavelengths of 655 nm and 665 nm, respectively. Moreover, we employed a linear transducer (L12-5) for the ultrasound imaging of the outlet channels (Vomark Technologies). The targeting performance of the system was evaluated using the Hemocytometer method. The targeting efficiency of the tested NK cell solution was determined to be 68% ± 2%.

4. CONCLUSIONS

In conclusion, this study demonstrated the capability of a

focused ultrasound beam to direct the movement of NK cells at vessel bifurcations, a technique with potential applications in immunotherapy. Additionally, we successfully simulated the relationship between the targeting efficiency and variables, such as cell size and fluid velocity. We observed that the efficiency diminished with smaller cell sizes and higher fluid velocities. However, this reduction in efficiency could be mitigated by incrementally increasing the intensity of the acoustic pressure. Our simulation model was experimentally validated using a phantom vessel bifurcation model that closely replicated the physical characteristics of actual vessels.

ACKNOWLEDGMENT

This research was supported by a grant from the Korean Health Technology R&D Project through the Korea Health Industry Development Institute (KHIDI), funded by the Ministry of Health & Welfare, Republic of Korea (Grant number: RS-2023-00302148).

REFERENCES

[1] H. Bruus, "Acoustofluidics 7: The acoustic radiation force on small particles", *Lab Chip*, Vol. 12, No. 6, pp. 1014-1021, 2012.

[2] S. Madersbacher, M. Pedevilla, L. Vingers, M. Susani, and M. Marberger, "Effect of high-intensity focused ultrasound on human prostate cancer in vivo", *Cancer Res.*, Vol. 55, No. 15, pp. 3346-3351, 1995.

[3] O. Al-Bataineh, J. Jenne, and P. Huber, "Clinical and future applications of high intensity focused ultrasound in cancer", *Cancer Treat. Rev.*, Vol. 38, No. 5, pp. 346-353, 2012.

[4] C. G. Chaussy and S. Thüroff, "High-Intensity Focused Ultrasound for the Treatment of Prostate Cancer: A Review", *J. Endourol.*, Vol. 31, No. S1, pp. S30-S37, 2017.

[5] J. E. Lingeman, J. A. McAteer, E. Gnessin, and A. P. Evan, "Shock wave lithotripsy: advances in technology and technique", *Nat. Rev. Urol.*, Vol. 6, No. 12, pp. 660-670, 2009.

[6] S.-M. Lee, N. Collin, H. Wiseman, and J. Philip, "Optimisation of shock wave lithotripsy: a systematic review of technical aspects to improve outcomes", *Transl. Androl. Urol.*, Vol. 8, No. 4, pp. S389(1)-S389(9), 2019.

[7] C. Cerrato, V. Jahrreiss, C. Nedbal, F. Ripa, V. De Marco, M. Monga, A. Pietropaolo, and B. Somani, "Shockwave Lithotripsy for De-Novo Urolithiasis after Kidney Transplantation: A Systematic Review of the Literature", *J. Clin. Med.*, Vol. 12, No. 13, pp. 4389(1)-4389(10), 2023.

[8] M. Sagris, A. Tzoumas, D. G. Kokkinidis, G. Korosoglou, M. Lichtenberg, and G. Tzavellas, "Invasive and pharmacological treatment of deep vein thrombosis: A scoping review", *Curr. Pharm. Des.*, Vol. 28, No. 10, pp. 778-786, 2022.

[9] N. B. Smith, "Applications of ultrasonic skin permeation in transdermal drug delivery", *Expert Opin. Drug Deliv.*, Vol. 5, No. 10, pp. 1107-1120, 2008.

[10] A. E. Cohen and W. E. Moerner, "Method for trapping and manipulating nanoscale objects in solution", *Appl. Phys. Lett.*, Vol. 86, No. 9, p. 093109, 2005.

[11] G. Go, V. D. Nguyen, Z. Jin, J.-O. Park, and S. Park, "A Thermo-electromagnetically Actuated Microrobot for the Targeted Transport of Therapeutic Agents", *Int. J. Control Autom. Syst.*, Vol. 16, No. 3, pp. 1341-1354, 2018.

[12] H. X. Cao, D. Jung, H. S. Lee, V. D. Nguyen, E. Choi, B. Kang, J. O. Park, and C. S. Kim, "Holographic Acoustic Tweezers for 5-DoF Manipulation of Nanocarrier Clusters toward Targeted Drug Delivery", *Pharmaceutics*, Vol. 14, No. 7, pp. 1490(1)-1490(16), 2022.

[13] E. Thomas, J. U. Menon, J. Owen, I. Skaripa-Koukelli, S. Wallington, M. Gray, C. Mannaris, V. Kersemans, D. Allen, P. Kinchesh, S. Smart, R. Carlisle, and K. A. Vallis, "Ultrasound-mediated cavitation enhances the delivery of an EGFR-targeting liposomal formulation designed for chemo-radionuclide therapy", *Theranostics*, Vol. 9, No. 19, pp. 5595-5609, 2019.

[14] C.-Y. Ting, C.-H. Fan, H.-L. Liu, C.-Y. Huang, H.-Y. Hsieh, T.-C. Yen, K.-C. Wei, and C.-K. Yeh, "Concurrent blood-brain barrier opening and local drug delivery using drug-carrying microbubbles and focused ultrasound for brain glioma treatment", *Biomaterials*, Vol. 33, No. 2, pp. 704-712, 2012.

[15] T. Ilovitsh, Y. Feng, J. Foiret, A. Kheirolomoom, H. Zhang, E. S. Ingham, A. Ilovitsh, S. K. Tumbale, B. Z. Fite, B. Wu, M. N. Raie, N. Zhang, A. J. Kare, M. Chavez, L. S. Qi, G. Pelled, D. Gazit, O. Vermesh, I. Steinberg, S. S. Gambhir, and K. W. Ferrara, "Low-frequency ultrasound-mediated cytokine transfection enhances T cell recruitment at local and distant tumor sites", *Proc. Natl. Acad. Sci. USA*, Vol. 117, No. 23, pp. 12674-12685, 2020.

[16] F. Fang, W. Xiao, and Z. Tian, "NK cell-based immunotherapy for cancer", *Semin. Immunol.*, Vol. 31, pp. 37-54, 2017.

[17] H. W. Song, H. S. Lee, S. J. Kim, H. Y. Kim, Y. H. Choi, B. Kang, C. S. Kim, J. O. Park, and E. Choi, "Sonazoid-Conjugated Natural Killer Cells for Tumor Therapy and Real-Time Visualization by Ultrasound Imaging", *Pharmaceutics*, Vol. 13, No. 10, pp. 1689(1)-1689(10), 2021.

[18] V. Bachanova, L. J. Burns, D. H. McKenna, J. Curtsinger, A. Panoskaltsis-Mortari, B. R. Lindgren, S. Cooley, D. Weisdorf, and J. S. Miller, "Allogeneic natural killer cells for refractory lymphoma", *Cancer Immunol. Immunother.*, Vol. 59, No. 11, pp. 1739-1744, 2010.

[19] M. Fan, M. Li, L. Gao, S. Geng, J. Wang, Y. Wang, Z. Yan, and L. Yu, "Chimeric antigen receptors for adoptive T cell therapy in acute myeloid leukemia", *J. Hematol. Oncol.*, Vol. 10, No. 1, pp. 151(1)-151(14), 2017.

[20] C. A. Ramos, H. E. Heslop, and M. K. Brenner, "CAR-T Cell Therapy for Lymphoma", *Annu. Rev. Med.*, Vol. 67, pp. 165-183, 2016.

[21] A. Merino, J. Maakaron, and V. Bachanova, "Advances in NK cell therapy for hematologic malignancies: NK source, persistence and tumor targeting", *Blood Rev.*, Vol. 60, p. 101073, 2023.

[22] E. Mylod, J. Lysaght, and M. J. Conroy, "Natural killer cell therapy: A new frontier for obesity-associated cancer", *Cancer Lett.*, Vol. 535, p. 215620, 2022.

[23] D. Murugan, V. Murugesan, B. Panchapakesan, and L. Rangasamy, "Nanoparticle Enhancement of Natural Killer (NK) Cell-Based Immunotherapy", *Cancers*, Vol. 14, No. 21, pp. 5438(1)-5438(24), 2022.

[24] M. J. Ko, H. Hong, H. Choi, H. Kang, and D. Kim, "Multifunctional magnetic nanoparticles for dynamic imaging and therapy", *Adv. NanoBio. Res.*, Vol. 2, No. 11, p. 2200053, 2022.

[25] S. Sharif, K. T. Nguyen, D. Bang, J.-O. Park, and E. Choi, "Optimization of Field-Free Point Position, Gradient Field and Ferromagnetic Polymer Ratio for Enhanced Navigation of Magnetically Controlled Polymer-Based Microrobots in Blood Vessel", *Micromachines*, Vol. 12, No. 4, pp. 424(1)-424(15), 2021.

[26] H. T. O'Neil, "Theory of focusing radiators", *J. Acoust. Soc. Am.*, Vol. 21, No. 5, pp. 516-526, 1949.

[27] L. P. Gor'kov, "On the forces acting on a small particle in an acoustical field in an ideal fluid", Vol. 6, pp. 773-775, 1962.

[28] L. R. Taggart, R. E. Baddour, A. Giles, G. J. Czarnota, and M. C. Kolios, "Ultrasonic characterization of whole cells and isolated nuclei", *Ultrasound Med. Biol.*, Vol. 33, No. 3, pp. 389-401, 2007.

[29] A. Zipursky, E. Bow, R. S. Seshadri, and E. J. Brown, "Leukocyte density and volume in normal subjects and in patients with acute lymphoblastic leukemia", *Blood*, Vol. 48, No. 3, pp. 361-371, 1976.

[30] J. Dahmani, C. Laporte, D. Pereira, P. Belanger, and Y. Petit, "Predictive Model for Designing Soft-Tissue Mimicking Ultrasound Phantoms With Adjustable Elasticity", *IEEE Trans. Ultrason. Ferroelectr. Freq. Control*, Vol. 67, No. 4, pp. 715-726, 2020.